Supporting information

Ultralow Flexural properties of Copper Microhelices Fabricated via Electrodeposition-based Three-Dimensional Direct-writing Technology

Zhiran Yi, Yu Lei, Xianyun Zhang, Yining Chen, Jianjun Guo, Gaojie Xu, Min-Feng Yu and Ping Cui*

Dr. Zhiran Yi, Miss Yu Lei, Mr Xianyun Zhang, Prof. Jianjun Guo, Prof. Gaojie Xu and Prof. Ping Cui
Zhejiang Key Laboratory of Additive Manufacturing Materials, Ningbo Institute of Materials Technology and Engineering, Chinese Academy of Sciences, Ningbo 315201, China
E-mail: jjguo@nimte.ac.cn

Miss Yu Lei
School of Materials Science and Engineering, Shanghai University, Shanghai 200444, China

Dr. Yining Chen and Prof. Min-Feng Yu
D. Guggenheim School of Aerospace Engineering, Georgia Institute of Technology, Atlanta, GA 30332, USA

S1. MCED fabricating process for microhelices

S1.1 Fabricating process for microhelices

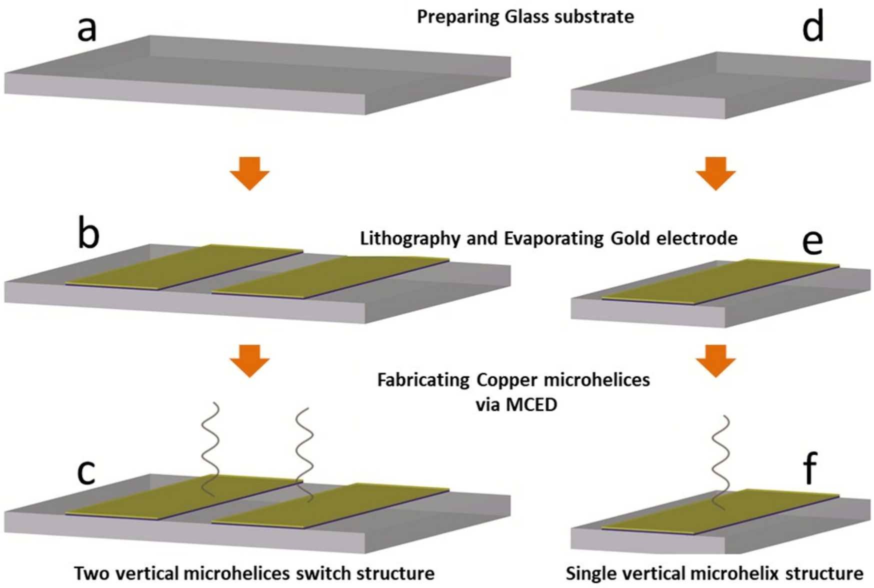

Figure S1. Fabricating process for microhelices. (a) and (d) Clean glass for substrate. (b) and (e) The gold thin film is coated by UV photolithography and e-beam evaporation technology. (c) Two micohelices are grown on two gold electrodes respectively. (f) A single microhelix is grown on the gold electrode.

S2.2 Fabricating copper microhelices via MCED

The direct writing process of a single microhelix can be divided into two steps. Firstly, the micropipette contacts with the substrate slowly due to the high-precision nanopositioning stage moving up. In order to avoid damaging the micropipette, the first step is relatively slow and generally it need to take about 7-10 minutes. Then, the microhelix is deposited at the substrate and the nanopositioning stage starts to move down at the same time. At this process, the nanopositioning stage is moved with a linear velocity of 0.13 μm/s along the circular arc of 5 μm diameter at the plane of XY and a linear velocity of 0.16 μm/s along the Z axis (the coordinate system shown in Figure S2). The coordinate system is shown in Figure S2. The high-precision nanopositioning system and the DC power system are controlled by LabVIEW. The DC power system is set with a constant current at 2.8~6.0 nA, which the microhelices diameter range from 0.8~1.6 μm. The varied voltage value is used as a trigger condition to convert different steps. Number of helical turns can be customized. Figure S3 shows some microphotographs of fabricating process of microhelices switch structure.

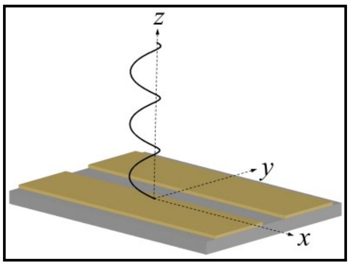

Figure S2 The coordinate system of fabricating process.

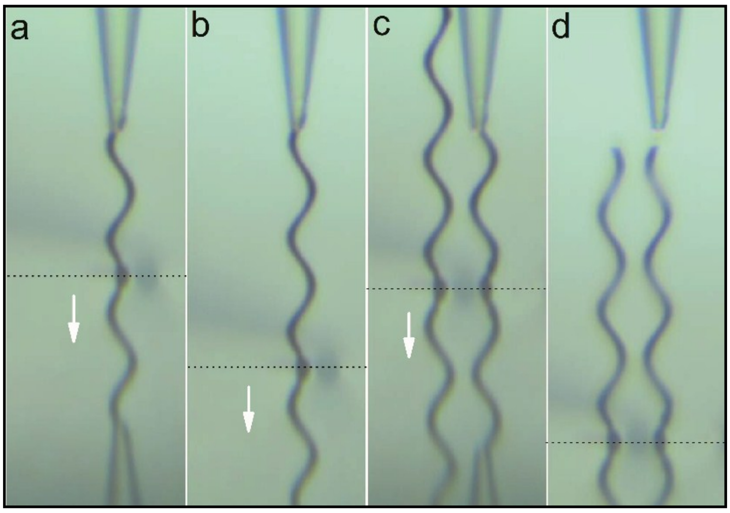

Figure S3 The microphotographs of fabricating process of microhelices switch structure.

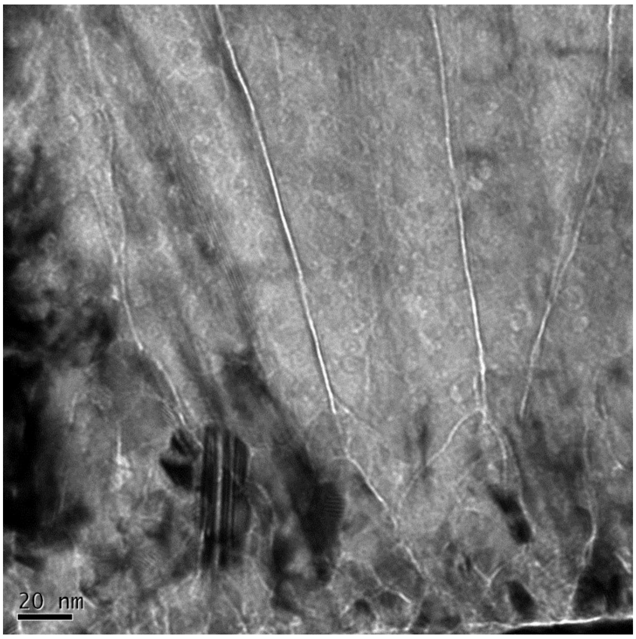

Figure S4 The TEM image of copper microwires fabricated by MCED

S2. Analytical description of microhelix bending

S2.1 Analytical models for the bending behavior of a helical wire

For the lateral vibration of helical spring, the spring subjecting to transverse force and bending moment is schematically shown in Fig.S5, where p is the pitch, Φ is the mean helical diameters, H is the axial free length, l is the total length of the wire, r is the weight density of Cu wires, $A=\pi d^2/4$ is the wire cross section area, t is time and θ is the polar coordinate of the spring. The following equation can be written:

$$H = l \cdot \sin\alpha = \frac{n\pi D}{\cos\alpha}\sin\alpha \qquad \text{(S1)}$$

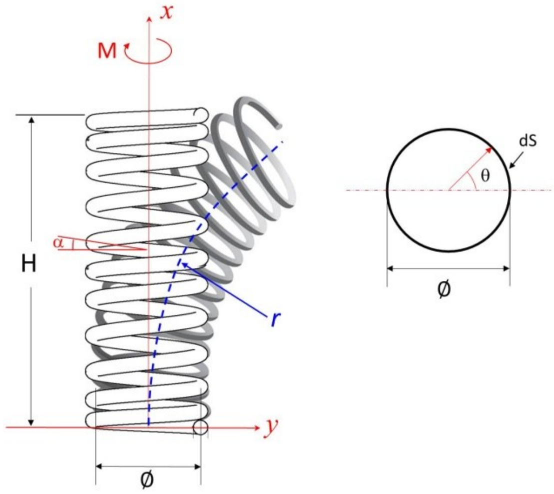

Figure S5 Bending of a helical spring

Under the assumption of using wire with circular cross-section and linear deformation, the work done by the torque M can be written as

$$U = \frac{1H}{2r}M \tag{S2}$$

when the axially helical spring loaded by a distributed load, a curvature radius r originates only from helix bending. Considering a differential length $ds= \Phi \cdot d\theta/2cos\alpha$ along centerline of wire helix, the total potential energy of the spring is found by carrying out the following integration:

$$W = \int_0^{2n\pi}\left[\frac{sin^2\theta sin^2\alpha + cos^2\theta}{2EI} + \frac{sin^2\theta sin^2\alpha}{2GJ}\right]M^2 ds \tag{S3}$$

Since U=W and $\frac{1}{r} = \frac{dy^2}{dz^2}$, Eqs. (S2) and (S3) can be reduced to

$$\frac{d^4y}{dx^4} = \frac{q}{sin\alpha}\left[\frac{1 + sin^2\alpha}{2EI} + \frac{cos^2\alpha}{2GJ}\right] \tag{S4}$$

where the inertial force q can be written as

$$q = -\frac{A\rho l}{H}\cdot\frac{\partial^2 y}{\partial t^2} \tag{S5}$$

By substituting Eqs. (S5) into Eqs. (S4),

$$\frac{d^4y}{dx^4} =-\frac{1}{sin\alpha}\left[\frac{1 + sin^2\alpha}{2EI} + \frac{cos^2\alpha}{2GJ}\right]\frac{A\rho l}{H}\cdot\frac{\partial^2 y}{\partial t^2} \tag{S6}$$

For a helix fixed at one end and free at another, as shown in Fig. S1, the boundary conditions at the fixed end (x=0) are

$$y = 0 \qquad and \qquad \frac{\partial y}{\partial x} = 0 \qquad (x = 0)$$

the boundary conditions at the fixed end (x=H) are for

$$\frac{\partial^2 y}{\partial x^2} = 0 \qquad and \qquad \frac{\partial^3 y}{\partial x^3} = 0 \qquad (x = H)$$

By solving Eq. (6), the bending vibration frequency can be obtained by

$$f = -\frac{k_i^2 H}{2\pi l}\sqrt{\frac{1}{A\rho\left[\frac{1+sin^2\alpha}{2EI}+\frac{cos^2\alpha}{2GJ}\right]}} \tag{S7}$$

Combining Eq. (3) with Eq. (S7), the flexural rigidity also can be calculated by:

$$f = -\frac{k_i^2 H}{2\pi l}\sqrt{\frac{K_1 l}{A\rho H}} \tag{S8}$$

$$K_1 = \frac{(2\pi f)^2 A\rho l}{k_1^4 H} \tag{S9}$$

Fig. S6 gives an example of the computed response curve for the resonance of a copper microhelix with 1.1 μm diameter at its fundamental mode. The intrinsic frequency is about 125 kHz.

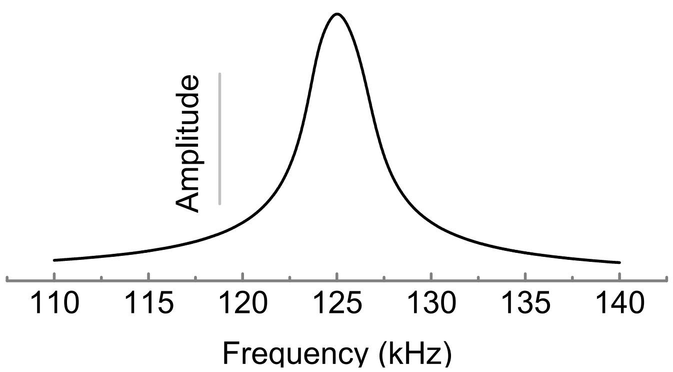

Figure S6 The computed response curve for the resonance of a copper microhelix with 1.1 μm diameter at its fundamental mode. The intrinsic frequency is about 125 kHz.

S2.2 The flexural rigidity obtained by analyzing the dynamic resonance behavior of single copper microhelix

$$K = \frac{(2\pi f)^2 A\rho l}{k^4 H} = \frac{(2\pi f)^2 \pi (D/2)^2 \rho \times \pi\phi n \times \sqrt{1+\frac{H^2}{(\pi\phi n)^2}} \times H^3}{(kH)^4}$$

$$= \frac{(2\times 3.14\times 123\times 10^3)^2 \times 3.14 \times (\frac{1.1}{2}\times 10^{-6})^2 \times 8960 \times 3.14 \times 5\times 10^{-6} \times 3 \times \sqrt{1+\frac{58^2}{(3.14\times 5\times 3)^2}} \times 58^3 \times 10^{-18}}{1.875^4} N\cdot \mathrm{m}^2$$

$$= 0.5989\times 10^{-14}\, N\cdot \mathrm{m}^2$$

S2.3 Effects of Wire Diameter on Flexural Rigidity

(1) Copper Microhelices

$$K=\frac{H}{l(\frac{1+\sin^2\alpha}{2EI}+\frac{\cos^2\alpha}{2GJ})}=\frac{2HEI\cos\alpha}{\pi\phi n(2+\mu\cos^2\alpha)}=\frac{HE\cos\alpha}{32\phi n(2+\mu\cos^2\alpha)}d^4$$

$$\tan\alpha=\frac{H}{n\pi\phi}$$

$$\cos\alpha=\frac{\pi\phi n}{\sqrt{H^2+(\pi\phi n)^2}}=\frac{3.14\times5\times3}{\sqrt{58^2+(3.14\times5\times3)^2}}=0.63$$

$$K=\frac{58\times10^{-6}\times120\times10^9\times0.63\times10^{-24}}{32\times5\times10^{-6}\times3\times(2+0.34\times0.63^2)}d^4=4.28\times10^{-15}d^4\ (N\cdot m^2)$$

By static deflections method, we obtain a flexural rigidity of 0.9×10^{-14} N·m^2 for microhelix with d=1.2 μm; By dynamic resonance method, the bending stiffness is 0.6 x10^{-14} N·m^2 for d=1.1 μm (see section 3.4). All these results fit well with the above theoretical relations. On the other way round, the dynamic resonance and deflections method can be used to estimate the mechanical properties of micro/nano-structures. We can obtain a Young's modulus of 115.8GPa for the MCED fabricated copper by Equ. (3). This agrees well with the nanoindentation results (119.5 GPa) and dynamic test of microwires (122.6 GPa, see Ref. 44).

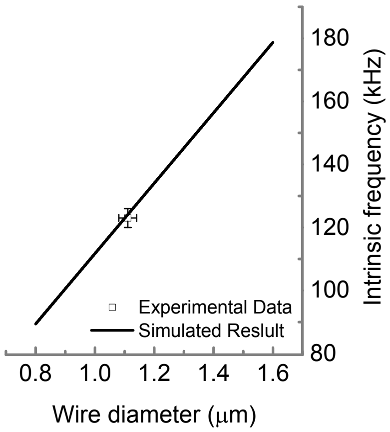

Figure S7. Effects of wire diameter on intrinsic frequency of copper microhelices

(2) Copper microwires

$$K=EI=\frac{120\times10^9\times\pi}{64}\times10^{-24}\times d^4=5.89\times10^{-15}d^4\ (N\cdot m^2)$$

S2.4 The Critical Load

According to the ***Theory of elastic stability***[1] discussed by Stephen P. Timoshenko and James M. Gere, we obtain the following equation for the critical load:

$$\frac{F_{cr}}{K}=\frac{1\pm\sqrt{1-\frac{4\pi^2K}{H^2B}(1-\frac{B}{A})}}{2(1-\frac{B}{A})}\times\frac{B}{K}$$

Where K, A and B respectively are flexural, shearing, and compressive rigidities of unloaded spring. In this study, the value of E/G is about 2.68, which corresponds to Poisson's ratio of 0.34.

$$K = \frac{2HEI\cos\alpha}{\pi\phi n(2+\mu\cos^2\alpha)},\ A = \frac{8HEI}{\pi\phi^3 n},\ B = \frac{8HGI}{\pi\phi^3 n}.$$

$$\frac{F_{cr}}{K} = \frac{1 - \sqrt{1 - \frac{\pi^2\phi^2\cos\alpha}{H^2(2+\mu\cos^2\alpha)}(1-\frac{G}{E})}}{2(1-\frac{G}{E})} \times \frac{4(2+\mu\cos^2\alpha)}{\phi^2\cos\alpha}$$

$$\frac{F_{cr}}{K} = (1 - \sqrt{1 - 6.1810\frac{\phi^2\cos\alpha}{H^2(2+0.34\cos^2\alpha)}}) \times \frac{5.3598(2+0.34\cos^2\alpha)}{\phi^2\cos\alpha}$$

S3. Comparison of mechanical properties for different microhelices

Table S1 Comparison of mechanical properties for different microhelices

Height(μm)	Pitch (μm)	Coil (μm)	Wire (μm)	Materials	Elastic stiffness (N/m)	References
20	2	0.84	0.12	Carbon	**0.12**	[2]
58	19.3	5	1.2	Copper	**0.13±0.01**	This work
6.3	1.2	1.6	0.2	tungsten-containing carbon (WC)	**0.9-1.5**	[3]
4.4	1.1	1.1	0.343	Si	**8.75±0.04**	[4]
2000	200	160	2.4	Si_3N_4	**0.32**	[5]
2000	500	800	150	CNT/Polymer Nanocomposite	**11.5**	[6]

References:

[1] S. P. Timoshenko, *Theory of elastic stability*. McGraw-Hill: **1961**; p 142.

[2] X. Chen,S. Zhang,D. A. Dikin,W. Ding,R. S. Ruoff,L. Pan,Y. Nakayama, *Nano Letters* **2003,** *3* (9), 1299-1304.

[3] K. Nakamatsu,J. Igaki,M. Nagase,T. Ichihashi,S. Matsui, *Microelectronic Engineering* **2006,** *83* (4-9), 808-810.

[4] J. P. Singh,D. L. Liu,D. X. Ye,R. C. Picu,T. M. Lu,G. C. Wang, *Applied Physics Letters* **2004,** *84* (18), 3657-3659.

[5] C. Cao,H. Du,Y. Xu,H. Zhu,T. Zhang,R. Yang, *Advanced Materials* **2008,** *20* (9), 1738-1743.

[6] L. L. Lebel,B. Aissa,M. A. El Khakani,D. Therriault, *Advanced Materials* **2010,** *22* (5), 592-596.